© 2018. Published by The Company of Biologists Ltd | Development (2018) 145, dev151548. doi:10.1242/dev.151548

RESEARCH ARTICLE

Tyrosine phosphorylation and proteolytic cleavage of Notch are required for non-canonical Notch/Abl signaling in *Drosophila* axon guidance

Ramakrishnan Kannan[1,*], Eric Cox[1,‡], Lei Wang[2,§], Irina Kuzina[1], Qun Gu[1] and Edward Giniger[1,2,¶]

ABSTRACT

Notch signaling is required for the development and physiology of nearly every tissue in metazoans. Much of Notch signaling is mediated by transcriptional regulation of downstream target genes, but Notch controls axon patterning in *Drosophila* by local modulation of Abl tyrosine kinase signaling, via direct interactions with the Abl co-factors Disabled and Trio. Here, we show that Notch-Abl axonal signaling requires both of the proteolytic cleavage events that initiate canonical Notch signaling. We further show that some Notch protein is tyrosine phosphorylated in *Drosophila*, that this form of the protein is selectively associated with Disabled and Trio, and that relevant tyrosines are essential for Notch-dependent axon patterning but not for canonical Notch-dependent regulation of cell fate. Based on these data, we propose a model for the molecular mechanism by which Notch controls Abl signaling in *Drosophila* axons.

KEY WORDS: Notch, Tyrosine phosphorylation, Proteolytic cleavage, Abl, Disabled, Trio, Axon guidance

INTRODUCTION

The receptor Notch and its associated signaling pathway are essential for the development of nearly every cell type in multicellular animals (Giniger, 2012; Greenwald and Kovall, 2013; Hansson et al., 2004). Upon activation by its ligands, Delta and Serrate, Notch undergoes a pair of proteolytic cleavages that release the intracellular domain (ICD) of the receptor (Kopan and Ilagan, 2009; Selkoe and Kopan, 2003), allowing it to transit to the nucleus and anchor the formation of a transcriptional activation complex that specifies the differentiated properties of a host of cell types. This signaling mechanism has been analyzed exhaustively because of its central importance for development and physiology throughout metazoan phylogeny.

Evidence has also accumulated, however, for the existence of 'non-canonical' signaling mechanisms for Notch (Andersen et al., 2012; Giniger, 2012). These include, for example, postulated interactions with components of the Wnt signaling pathway (Hayward et al., 2005) and the Akt pathway (Androutsellis-Theotokis et al., 2006; Perumalsamy et al., 2009), among others, that extend the menu of molecular outcomes of Notch activation. The molecular events behind these alternative signaling mechanisms, however, are not well understood.

Perhaps the best-studied non-traditional function of Notch is its regulation of axon patterning (comprising both axon growth and axon guidance) via interaction with the Abl tyrosine kinase signaling network (Crowner et al., 2003; Giniger, 1998; Kuzina et al., 2011; Le Gall et al., 2008). It has been demonstrated biochemically, molecularly and genetically that, upon activation by its ligand Delta, Notch promotes the growth and guidance of pioneer axons in the *Drosophila* embryo by locally suppressing Abl signaling (Crowner et al., 2003; Giniger, 1998; Kuzina et al., 2011). Notch binds *in vivo* to two upstream components of the Abl pathway (Le Gall et al., 2008), namely the adapter protein Disabled (Dab), which localizes Abl protein and stimulates its kinase activity (Kannan et al., 2017; Song et al., 2010), and the guanine exchange factor (GEF) Trio, which activates Abl-dependent signaling by Rac GTPase (Newsome et al., 2000). Genetic experiments demonstrated that these molecular interactions with components of the Abl pathway mediate the axon patterning function of Notch but not its cell fate function. Most informatively, molecular studies have generated mutant forms of Notch that disrupt the direct binding site for Dab and are selectively impaired for the Notch axon guidance function but active in cell fate control, and, conversely, forms that are selectively impaired in cell fate control but active in axon patterning, notably a form that lacks the binding sites for the canonical transcriptional effector Su(H) (Le Gall et al., 2008). Together, these data provided compelling evidence that the Abl-dependent axon patterning function of Notch employs a unique signaling mechanism that is molecularly distinct from the canonical Notch signaling machinery. A related Notch signaling machinery evidently exists in mammals, where the Notch-Disabled interaction is a key link in reelin-dependent lamination of the cortex during brain development (Hashimoto-Torii et al., 2008; Keilani and Sugaya, 2008; Sibbe et al., 2009).

We now dissect the molecular mechanism of the Notch/Abl signaling pathway, and in particular its relationship to the mechanism of canonical Notch signaling. We first show that regulation of Abl-dependent axon patterning requires both of the ligand-induced proteolytic cleavages of Notch, namely S2 cleavage of the extracellular domain and Presenilin-mediated intramembranous S3 cleavage, and also that both Trio and Dab proteins associate with Notch both before and after ligand activation. We then map more precisely the Dab binding site on the Notch ICD and show by mutation that it is required for the complete axon patterning function of Notch but not for regulation of neuronal identity. Finally, we show that *Drosophila* Notch is tyrosine-phosphorylated *in vivo*, that the

[1]National Institute of Neurological Disorders and Stroke, National Institutes of Health, Bethesda, MD 20892, USA. [2]Fred Hutchinson Cancer Research Center, 1100 Fairview Ave, N., Seattle, WA 98109, USA.
*Present address: Neurobiology Research Center (NRC), Department of Psychiatry, National Institute of Mental Health and Neurosciences, Bangalore-40, India. ‡Present address: National Library of Medicine, National Institutes of Health, Bethesda, MD 20892, USA. §Present address: St. Jude Children's Research Hospital, Department of Developmental Neurobiology, Memphis, TN 38105, USA.

¶Author for correspondence (ginigere@ninds.nih.gov)

R.K., 0000-0001-7717-0516; E.G., 0000-0002-8340-6158

Received 3 March 2017; Accepted 08 December 2017

Development (2018) 145, dev151548. doi:10.1242/dev.151548

tyrosine-phosphorylated form of the protein is selectively associated with Dab and Trio, and that relevant tyrosines are necessary for complete axonal function *in vivo*, but not for canonical Notch activity. Based on these data we propose a molecular model for the mechanism by which a tyrosine-phosphorylated population of Notch protein molecules suppresses Abl signaling in *Drosophila* axons.

RESULTS

Ligand-induced proteolytic cleavage of Notch is required to regulate axon patterning

Genetic and molecular experiments argue that regulation of axon patterning by Notch requires both the S2 and S3 proteolytic cleavages of the receptor. A dominant-negative form of the S2 protease Kuzbanian causes breaks in central nervous system (CNS) longitudinal tracts reminiscent of *Notch* mutant phenotypes (Fambrough et al., 1996), but these effects are difficult to interpret since Kuzbanian also processes other cell surface proteins that contribute to these same axon patterning decisions (Coleman et al., 2010; Hattori et al., 2000). We therefore sought a more specific reagent to assess the role of S2 cleavage in Notch axonal activity. The Notch glucosylase Rumi has been characterized extensively in *Drosophila* (Acar et al., 2008). Rumi-dependent modification of Notch is absolutely and selectively required for S2 cleavage of the receptor at elevated temperature (30°C), but not at 25°C. In a wild-type genetic background, Rumi modification apparently is not essential for any other step of Notch activation or function and Rumi acts on few other proteins in *Drosophila* (see the Discussion for more detailed consideration of Rumi as a reagent to manipulate Notch cleavage). We therefore used germline clones to prepare embryos that were mutant for *rumi* both maternally and zygotically, and raised the temperature after CNS neurogenesis is largely complete but prior to a *Notch*-dependent axon patterning decision, namely the defasciculation of ISNb motoneurons. Under these conditions, neuronal fate and differentiation are largely normal, and we could test for a selective requirement for S2 cleavage during ISNb growth.

The ISNb motonerve comprises eight motor axons that innervate seven ventrolateral bodywall muscles (Fig. 1D). ISNb axons exit the CNS in the intersegmental nerve (ISN), but in response to Delta protein at a peripheral choice point, ISNb axons defasciculate from the ISN to enter their target muscle field (Crowner et al., 2003). In the absence of Delta at the choice point, or of Notch activation in the neurons, ISNb axons fail to defasciculate, and continue growing in the ISN. This is termed a 'bypass' of the defasciculation point (Wills et al., 1999). We now found that in embryos lacking *rumi* activity at the time of ISNb defasciculation, ISNb displays the characteristic *Notch* bypass phenotype in 59±2% of hemisegments [n=119; observed in <1% of hemisegments in wild type (Crowner et al., 2003)] (Fig. 1A,B).

There are very few cell surface proteins in *Drosophila* that bear the consensus glucosylation target sequence for Rumi, and consistent with this the *rumi* phenotype is an excellent proxy for the *Notch* phenotype (Acar et al., 2008). Nonetheless, to rule out the possibility that there might be another Rumi-dependent receptor involved in ISNb patterning we took advantage of transgenic *Notch* derivatives, expressed from the wild-type *Notch* promoter, that have been engineered to make the receptor Rumi-insensitive by mutating potential Rumi target sites in the Notch coding sequence (Leonardi et al., 2011; see Materials and Methods for details). The modified transgene rescues a *Notch* mutant at low temperature, where Rumi-dependent modification of Notch is not required, but not at elevated temperature, where Rumi activity is essential for S2 cleavage of Notch (Leonardi et al., 2011).

We performed the ISNb temperature shift on embryos expressing the *rumi*-insensitive $Notch^{gt\ 10\text{-}20}$ in the background of the null allele $Notch^{5419}$. Examination of ISNb demonstrated a high frequency of the characteristic *Notch* ISNb bypass phenotype (62±7%; n=162 hemisegments; Fig. 1C), confirming the specific requirement for Notch to be modified by Rumi in order to execute ISNb axon guidance at elevated temperature. We further verified that this defect in ISNb is not secondary to alterations of *Notch*-dependent identity or differentiation of the motoneurons or their target muscles. Disruption of *Notch*-dependent muscle development blocks myoblast fusion and disrupts muscle morphology (Fuerstenberg and Giniger, 1998). Muscle morphology appears wild type, however, in our temperature-shifted embryos (Fig. 1B,C), excluding *Notch*-dependent defects in the fates of ISNb target muscles. Regarding neuronal identity, all ISN neurons, and no ISNb neurons, express the transcription factor Even-skipped (Eve), which is a direct regulator of guidance molecules required for ISN targeting (Labrador et al., 2005). Therefore, if the bypass of ISNb axons in these experiments was due to alteration of neuronal cell identities, it would be accompanied by misexpression of Eve in motoneurons RP1, 3, 4 and 5. We therefore stained collections of temperature-shifted $Notch^{5419}$; $Notch^{gt\ 10\text{-}20}$ embryos with anti-Eve antibody. Out of 96 hemisegments examined, (containing 384 RP1, 3, 4 and 5 neurons), we detected only three cases of a single supernumerary Eve^{+} nucleus near the position of the RP motoneuron cell bodies (<1% of potentially affected cells; Fig. 1E). This cannot account for a bypass phenotype observed in >60% of ISNb hemisegments. Together, therefore, these experiments demonstrate that S2 cleavage is essential for *Notch*-dependent ISNb guidance.

We next examined the potential role of *Presenilin* (*Psn*)-dependent S3 cleavage in *Notch*-dependent axon patterning. Complete loss of maternal and zygotic *Psn* activity leads to severe developmental defects (Struhl and Greenwald, 1999), so we prepared $Notch^{ts1}$ embryos that were, or were not, heterozygous for either of two independent *Psn* null alleles, and assayed ISNb patterning under a temperature-shift protocol that produces a partial *Notch* loss-of-function phenotype in ISNb (Fig. 2A-C′, quantified in D). For both alleles tested, reduction of *Psn* gene dosage caused substantial enhancement of the *Notch* ISNb phenotype [ISNb bypass frequency of 31% (n=235 hemisegments) for $Notch^{ts1}$, versus 44% (n=180) for $Notch^{ts1}$; $Psn^{C2/+}$ (P<0.05), and 45% (n=194) for $Notch^{ts1}$; $Psn^{143/+}$ (P<0.01); significance by χ^2, with Bonferroni correction]. A heterozygous *Psn* mutation gives few axonal defects by itself (4.6%; n=131). These data argue that Psn-dependent (S3) cleavage of Notch is crucial for *Notch*-dependent axon patterning.

Association of Dab and Trio binding with Notch activity and cleavage

The Abl co-factors Dab and Trio associate with the ICD of Notch *in vivo* (Le Gall et al., 2008). The following experiments, however, show that this binding of Dab and Trio does not require activation of Notch signaling or binding of ligand. The $Notch^{ts1}$ mutant allele cannot be activated for signaling. We therefore raised $Notch^{ts1}$ animals at restrictive temperature (32°C), prepared extracts, and performed co-immunoprecipitation (co-IP) experiments. We found that in extracts prepared from tissue held at restrictive temperature, both Dab and Trio co-precipitate with Notch at least as effectively as they do in tissue raised at permissive temperature (18°C). This result was obtained both with extract from embryos (Fig. 3A) and from adult heads (Fig. 3B). To test specifically for ligand dependence of effector binding to Notch, we expressed a Notch derivative that lacks the Delta/Serrate-binding EGF repeats ($Notch^{\Delta 10\text{-}12}$) (Le Gall et al., 2008; Rebay et al., 1993; Zecchini et al., 1999), and again

Development (2018) 145, dev151548. doi:10.1242/dev.151548

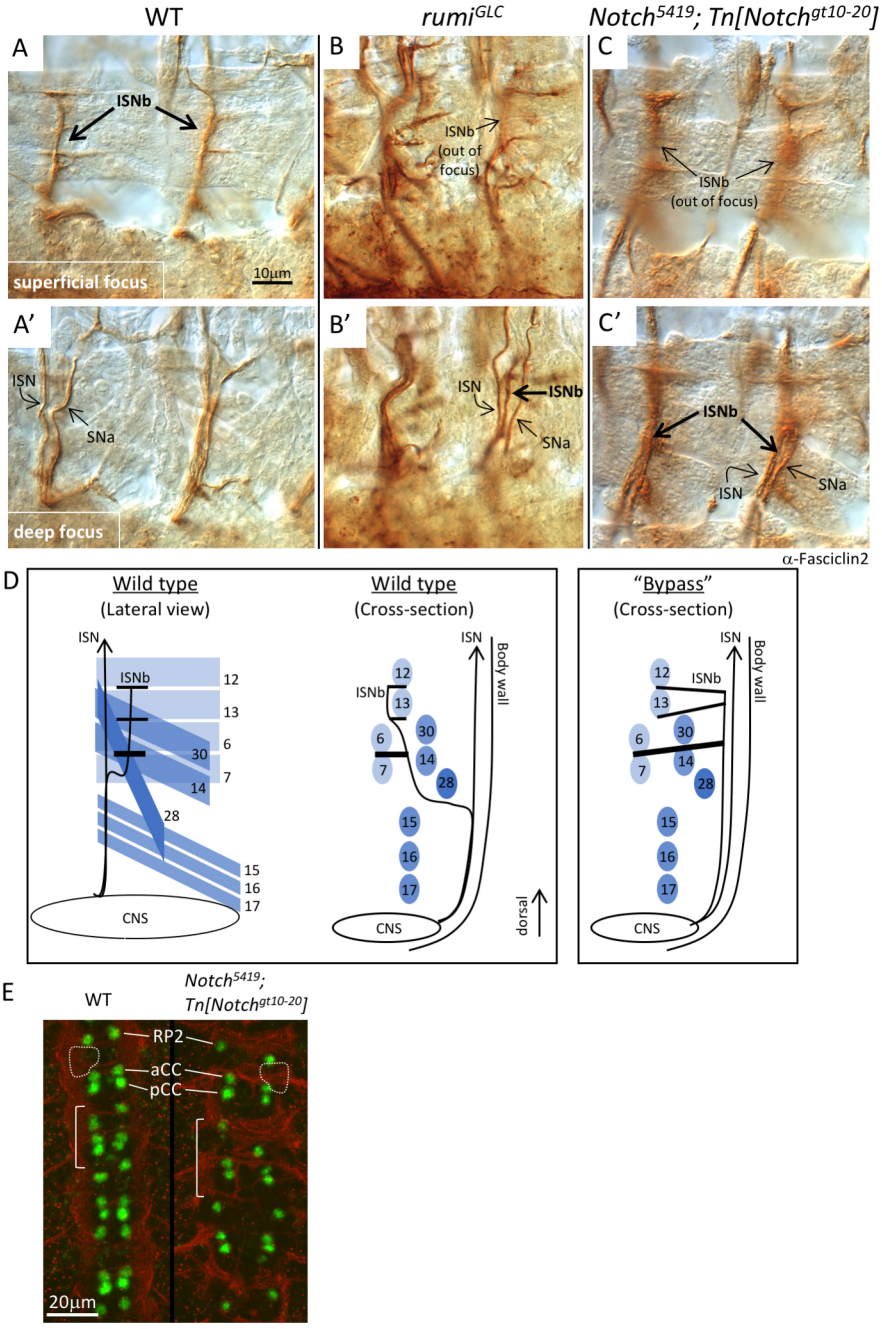

Fig. 1. Rumi glucosylation of Notch is required for ISNb defasciculation. (A-C′) *Drosophila* embryos were collected at 18°C, shifted to 32°C, fixed and immunostained with anti-Fasciclin 2 for peroxidase histochemistry. ISNb was visualized by Nomarski microscopy. Lateral views of two hemisegments are shown at two planes of focus: superficial (A-C) and deep (A′-C′). In wild type (WT; A,A′), ISNb is in focus in the superficial focal plane; in mutant embryos with a 'bypass' phenotype, the misrouted ISNb is in focus in the deep focal plane. (B,B′) *rumi*^{26} homozygous mutant from *rumi*$^{-/-}$ germline clone (GLC). (C,C′) *Notch*^{5419} null embryo carrying a *Notch* genomic transgene (*Notch*$^{gt\ 10\text{-}20}$) that lacks Rumi glucosylation sites. (D) Schematic of ISN/ISNb anatomy. Left two panels represent wild-type anatomy; right panel depicts a 'bypass' hemisegment. ISN runs dorsally from the CNS. In wild type, ISNb defasciculates from the ISN ventral to muscles 14 and 28 to enter the ventrolateral muscle field, and forms synapses. In a bypass hemisegment, ISNb axons ignore the defasciculation point and continue to project in the ISN. Abdominal muscles are represented as blue rectangles and trapezoids in the lateral view and as ovals in the cross-sections, and are identified with numbers; they are color-coded by depth in the embryo, with the most internal muscles the lightest color. Black lines represent ISN and ISNb; horizontal black bars represent synapses to ventral longitudinal muscles. Synapses to oblique muscles have been omitted for clarity. Dorsal is at the top. (E) Effect of Rumi modification of Notch on cell fates in the dorsal CNS. Embryos were subjected to temperature shift, fixed, and labeled with anti-Eve (green) and anti-HRP (red; to visualize neuropil). A maximum intensity projection is shown of tissue that includes RP1, 3, 4 and 5; these lie between, and slightly lateral to, RP2 and aCC (region indicated by the dotted outline). RP2, aCC and pCC are labeled in one hemisegment of each image. No supernumerary Eve^{+} neurons are visible in the positions of RP neurons in this mutant embryo. Bracket indicates approximate extent of one segmental ganglion. Scale bars: 10 µm in A-C′; 20 µm in E.

performed co-IP (Fig. 3C). We found that anti-Trio co-precipitated Notch$^{\Delta 10\text{-}12}$ as effectively as it co-precipitates wild-type Notch. Together, these experiments show that association of Notch with its partners *in vivo* does not depend on ligand activation of signaling.

Next, we tested whether Dab and Trio bind to activated forms of Notch, or only to the full-length protein prior to ligand binding. We expressed in *Drosophila* embryos a constitutively active form of Notch lacking its extracellular domain [*FLAG-Notch*$^{\Delta E}$ (Larkin et al., 1996)] and performed co-IP (Fig. 3D,E). We found that both Dab and Trio co-precipitate efficiently with the constitutively active Notch$^{\Delta E}$, demonstrating that these proteins remain bound to Notch even after ligand activation. The gel system does not distinguish Notch$^{\Delta E}$ from its S3-cleaved product, Notch^{intra}, but previous studies of mammalian Notch have documented *in vivo* binding of disabled 1 (Dab1) to Notch^{intra} in mouse cells (Hashimoto-Torii et al., 2008; Sibbe et al., 2009). Therefore, we also used co-IP to test binding of Dab to Notch ICD (NICD$^{\Delta 2155}$, expressed with *elav-GAL4*). As expected, the efficiency of Dab-NICD co-precipitation was extremely low since, unlike the membrane-tethered Notch$^{\Delta E}$, only a tiny fraction of expressed NICD is present outside the nucleus and thus available to associate with Dab (Le Gall and Giniger, 2004). Nonetheless, co-IP of Dab with Notch was detected consistently, albeit weakly (Fig. 3F; observed in 5 biological replicates). We were not able to assay co-precipitation of NICD with Trio in this experiment due to non-specific association of Trio with anti-FLAG beads.

Mapping and function of the Dab binding site on Notch

Previous studies demonstrated that a portion of the juxtamembrane region of NICD is required for *in vitro* binding of Dab to Notch, and that deletion of this region compromises Notch axonal function

Development (2018) 145, dev151548. doi:10.1242/dev.151548

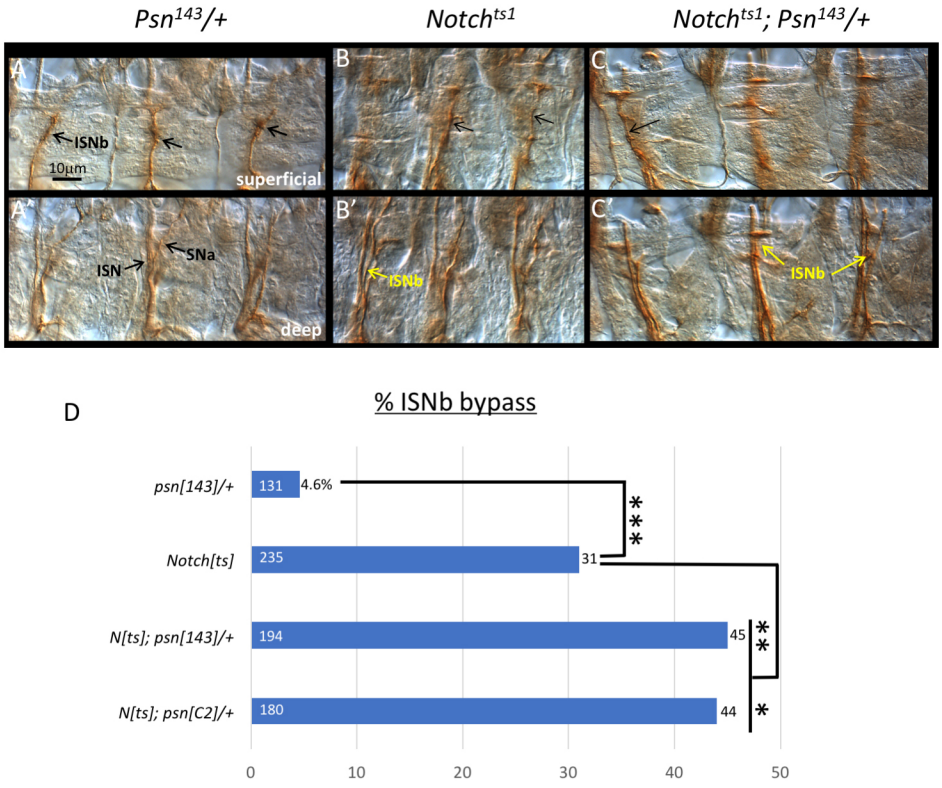

Fig. 2. *Notch* and *Presenilin* mutations interact synergistically to disrupt ISNb defasciculation. (A-C′) Embryos were collected, subjected to ISNb temperature shift, fixed, immunostained with anti-Fasciclin 2 and for peroxidase histochemistry and visualized by Nomarski microscopy. Lateral views of three hemisegments are shown in a superficial (A-C) and a deep (A′-C′) focal plane. (A,A′) ISNb is superficial, whereas ISN and SNa are deep in all three hemisegments; (B-C′) ISNb projects at the deep level in some hemisegments (bypass phenotype, indicated in yellow); thin black arrows indicate hemisegments with properly projecting (superficial) ISNb. Scale bar: 10 µm. (D) Graph showing bypass frequency in abdominal hemisegments 2-7 from the experiment of A-C′. **P*<0.05, ***P*<0.01, ****P*<0.001 (χ^2, with Bonferroni correction). Bypass frequency (black numbers) and *n* (white numbers) are indicated for each genotype.

(Le Gall et al., 2008; Le Gall and Giniger, 2004). In those experiments, however, the Dab binding site was mapped only to a broad region (36 codons), and the minimal deletion that impaired Notch axonal function also deleted one of the three Su(H) binding sites on Notch, complicating the interpretation of functional experiments. We therefore refined the mapping of the Dab binding site, and demonstrated more rigorously its selective requirement for Notch axonal function. In the experiments that first characterized the juxtamembrane domain of Notch (called the Ram domain), Honjo and co-workers identified five short sequence motifs that were conserved among Notch genes (Tamura et al., 1995). Motifs 1, 2 and 3 constitute the binding site for the transcriptional effector of Notch, RBP-Jκ [also called CSL or, in flies, Su(H)]. Motifs 4 and 5, by contrast, were not required for binding to RBP- Jκ *in vitro*, and are physically distant from the RBP-Jκ binding region in the NICD crystal structure (Wilson and Kovall, 2006) (Fig. 4A). Motifs 4 and 5, however, flank the C-terminal border of a portion of Notch that is crucial for Dab binding *in vitro*, a region called the Ram A domain (Le Gall and Giniger, 2004). We therefore prepared derivatives of *Drosophila Notch* lacking sequences homologous to motifs 4 and 5 and assayed binding of Dab *in vitro* and axon guidance and neurogenic function *in vivo*.

Deletion of Ram motifs 4 and 5 severely disrupts binding of Dab to NICD *in vitro* and the axonal function of Notch *in vivo*, but does not diminish the canonical neurogenic function of Notch *in vivo*. We prepared beads bearing the Dab phosphotyrosine-binding (PTB) domain linked to GST and found that they efficiently pull down the wild-type Notch Ram domain, but not Notch Ram$^{\Delta 4\text{-}5}$ (Fig. 4B). We then assayed the ability of Notch lacking these motifs to rescue the extension of CNS longitudinal axons and guidance of ISNb motor axons in *Notch^{ts}* embryos. The Δ4-5 deletion was introduced into the minimal *Notch* derivative that fully rescues *Notch* axonal function, placed under *GAL4* control (*UAS-Notch$^{\Delta 2155(\Delta 4\text{-}5)}$*), and expressed in neurons (with *elav-GAL4*). Relative to the parent *Notch* gene (*UAS-Notch$^{\Delta 2155}$*), in these assays *Notch$^{\Delta 2155(\Delta 4\text{-}5)}$* is impaired by ∼60% in its ability to suppress characteristic axon patterning defects in the CNS (Fig. 4D,E), and by ∼90% in its ability to suppress axonal defects of ISNb (Fig. 4C) of temperature-shifted *Notch^{ts1}* mutant embryos. Equivalent expression of these *Notch* transgenes was verified by western analysis (see Fig. 6E, input).

By contrast, it has been shown previously that mutation of motifs 4 and 5 does not disrupt binding of Notch to RBP-Jκ (Tamura et al., 1995), suggesting that it might not disrupt canonical Notch signaling. We therefore expressed either a longer *Notch* form that retains partial canonical signaling activity, *Notch$^{\Delta 2268}$*, or the Δ4-5 derivative of that form, *Notch$^{\Delta 2268(\Delta 4\text{-}5)}$*, in the background of a strong *Notch* allele and assayed the CNS hyperplasia phenotype that is the classic measure for defects in canonical Notch signaling in *Drosophila* [increased neuron number, assayed as CNS broadening (Lehmann et al., 1983; Lieber et al., 1993; Le Gall and Giniger, 2004)]. We found that CNS hyperplasia is suppressed by *Notch$^{\Delta 2268(\Delta 4\text{-}5)}$* at least as effectively as it is by *Notch$^{\Delta 2268}$*, confirming that the Δ4-5 deletion does not materially diminish canonical Notch signaling activity (Fig. 4F, see also Fig. 7A-D,F). Again, equivalent expression of the *Notch* transgenes was verified by western analysis (Fig. 6D).

Tyrosine phosphorylation of Notch is essential for full axonal function

Since the axon patterning function of Notch is mediated through interaction with core components of the Abl tyrosine kinase signaling pathway, we asked whether any components of this molecular machine are phosphorylated on tyrosine. To our surprise, we found that Notch itself is tyrosine phosphorylated in *Drosophila* embryos. Anti-phosphotyrosine westerns of anti-Notch immunoprecipitates show a faint but detectable high molecular weight phosphotyrosine-immunoreactive band that comigrates precisely with Notch in wild-type embryo extracts, and increased levels of this species in

Development (2018) 145, dev151548. doi:10.1242/dev.151548

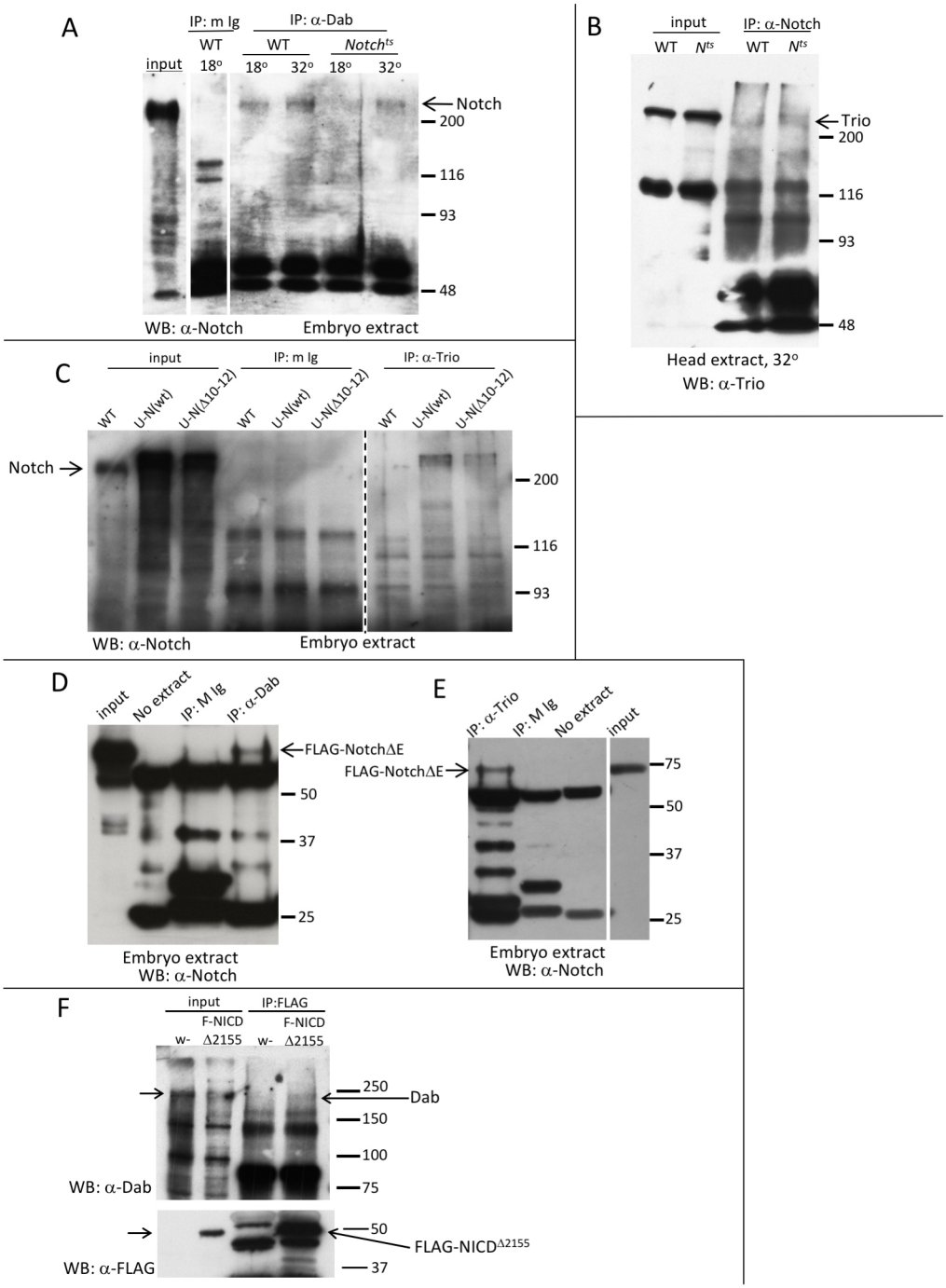

Fig. 3. Notch binds Dab and Trio regardless of activation state. Embryo or adult head extracts were subjected to co-immunoprecipitation (co-IP) and western analysis. Samples were separated by SDS-PAGE, transferred, and visualized by ECL. Positions of molecular weight markers are indicated (kDa). In some panels, irrelevant intervening lanes were excised from the images (white vertical lines). (A) Anti-Notch western, after precipitation with anti-Dab or mouse IgG control. Arrow indicates full-length Notch. Equal protein concentration of the extracts was verified by Ponceau staining of a parallel gel (not shown). (B) Anti-Trio western after precipitation with anti-Notch. Arrow indicates full-length Trio. (C) Anti-Notch western of immunoprecipitates from extract of wild-type embryos, or embryos overexpressing the indicated Notch derivative. Exposure was adjusted so that co-precipitation of endogenous Notch is at or below the limits of detection (lane 7), to ensure that UAS-Notch IP signals (lanes 8, 9) report the overexpressed transgenes. Samples were run on two parallel gels in a single buffer chamber (denoted by the vertical dashed line) and blots aligned based on markers. (D,E) Anti-Notch westerns of immunoprecipitates from extract of wild-type embryos expressing constitutively active Notch lacking its extracellular domain (FLAG-Notch$^{\Delta E;}$, arrow). (D) co-IP with anti-Dab; (E) co-IP with anti-Trio. (F) (Top) Anti-Dab western of anti-FLAG immunoprecipitates from extract of embryos that do or do not express *FLAG-NICD$^{\Delta 2155}$* under the control of *elav-GAL4*. Arrows point to the Dab band in the input lane and (faintly) in the FLAG-NICD IP lane; it is not present in the *w*– control IP lane. (Bottom) Anti-FLAG western of the same gel after stripping and reprobing. Arrows indicate position of FLAG-NICD$^{\Delta 2155}$.

extracts of Notch-overexpressing embryos (UAS-N; Fig. 5A). Consistent with this, immunoprecipitation (IP) of phosphotyrosine-containing proteins performed at high stringency (in the presence of 0.1% SDS to disrupt protein complexes) precipitated Notch protein (Fig. 5B). Finally, treatment of anti-Notch immunoprecipitates with alkaline phosphatase eliminated the anti-phosphotyrosine signal, verifying that it reflects authentic phosphorylation (Fig. 5C). We therefore infer that Notch is phosphorylated on tyrosine residues in *Drosophila* embryos.

We next tested whether the population of Notch protein molecules present in complexes with Dab and Trio bears the phosphorylated tyrosine. We found not only that tyrosine-phosphorylated Notch is present in Dab and Trio complexes, but also that it is included preferentially, if not exclusively, in these complexes. IP of embryo extracts with anti-Dab or anti-Trio and western analysis of serial dilutions demonstrated that ∼5% of the total Notch in the extract co-precipitated with Dab or Trio [Fig. 5D, bottom; quantification estimated based on comparison of band intensities, corrected for dilution and IP efficiency (measured independently)]. Remarkably, however, this population of Notch protein included essentially all of the anti-phosphotyrosine immunoreactivity we could detect in anti-Notch immunoprecipitates, i.e. essentially all of the tyrosine-phosphorylated Notch in the sample (Fig. 5D, top). Stated otherwise, the Notch protein in Dab- or Trio-immunoprecipitable complexes was enriched ∼20-fold

Development (2018) 145, dev151548. doi:10.1242/dev.151548

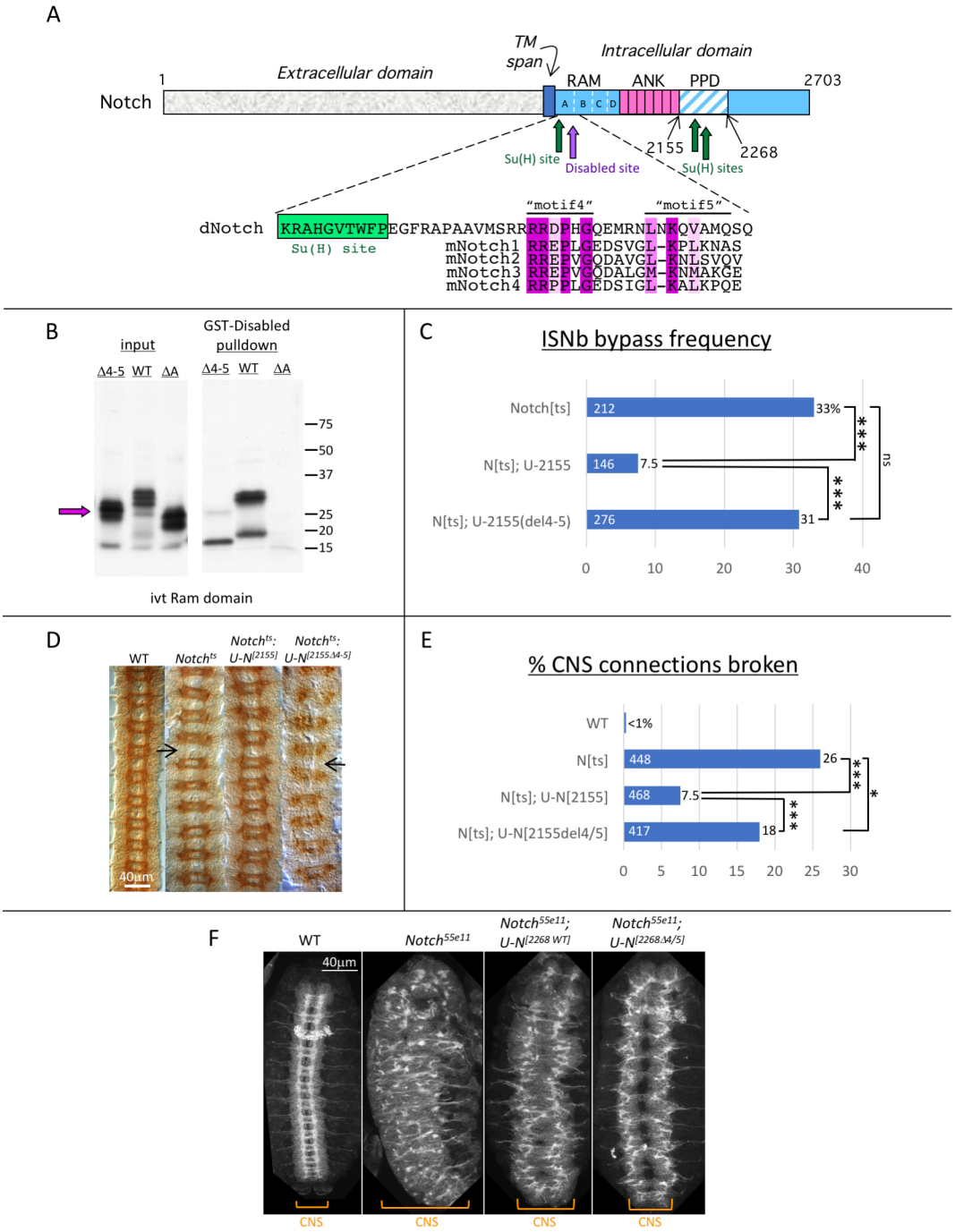

Fig. 4. Deletion of the Dab binding site selectively disrupts Notch axonal function. (A) Alignment of a portion of *Drosophila* (d) *Notch* with conserved motifs 4 and 5 from mouse (m) *Notch1-4* (Tamura et al., 1995). (B) GST-Dab(PTB) domain was used to pull down the indicated *in vitro* translated derivatives of the Notch Ram domain (arrow). Reduced pulldown of mutant derivative was observed in two independent experiments, and the equivalent result was observed in the inverse experiment, using bead-immobilized Notch derivatives to pull down *in vitro* translated Dab (data not shown). (C) ISNb bypass frequency in the indicated genotypes. ns, not significant; ***P<0.001 (χ^2, with Bonferroni correction). White numbers indicate n for each genotype. Expression of *Notch* derivatives was driven with *P[elav-GAL4]*. (D) Dorsal view of CNS axon tracts in temperature-shifted stage 17 embryos, as revealed by peroxidase immunohistochemistry with mAb BP102. Examples of breaks in longitudinal axon tracts between successive segments are indicated (arrows). Transgene expression was driven with *P[elav-GAL4]*. (E) Quantification of longitudinal tract breaks in the experiment of D. *P<0.05, ***P<0.001 (χ^2, with Bonferroni correction). White numbers indicate n. (F) Ventral view of CNS neurons visualized by immunofluorescence with anti-HRP. Width of the CNS (reflecting total number of neurons) for the indicated genotypes is indicated with an orange bracket. Expression of *Notch* derivatives was driven with *sca-GAL4*. Scale bars: 40 μm.

in tyrosine-phosphorylated Notch relative to the total Notch protein in the starting extract. This suggests that most, possibly all, of the tyrosine-phosphorylated Notch in fly embryos is associated with Dab and Trio.

Directed mutagenesis of Notch and functional assay of the resulting derivatives suggests that tyrosine phosphorylation of NICD is essential for full activity in axon patterning, but not for neuronal cell fate control. As shown previously (Le Gall et al.,

Development (2018) 145, dev151548. doi:10.1242/dev.151548

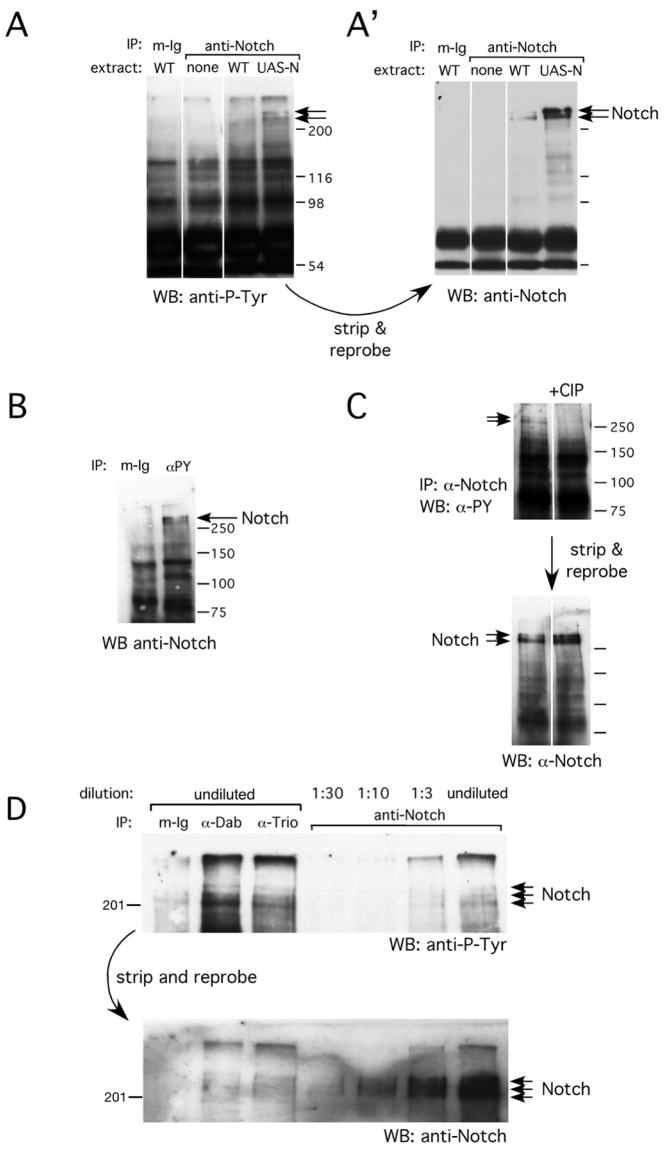

Fig. 5. Notch is tyrosine-phosphorylated *in vivo*. (A) Western blot of embryo immunoprecipitates, probed with anti-phosphotyrosine (mAb 4G10). Arrows indicate a pair of high molecular weight bands detected in immunoprecipitates of samples overexpressing Notch, and faintly in IP of wild type, but not in controls. (A′) Same filter, stripped and reprobed with anti-Notch. Full-length Notch comigrates with the anti-phosphotyrosine signal from A. Observations shown are representative of at least five experiments. (B) Western blot of anti-phosphotyrosine IP of wild-type embryos, probed with anti-Notch. Arrow indicates wild-type Notch. (C) (Top) Anti-phosphotyrosine western blot of anti-Notch IP of extracts from embryos that overexpressed full-length wild-type Notch. Extracts were, or were not, treated with calf intestine phosphatase (CIP). (Bottom) Stripping the filter and reprobing with anti-Notch documents that the phosphatase-sensitive products comigrate with wild-type Notch. Observations were reproduced in four experiments. (D) (Top) Embryos overexpressing full-length wild-type Notch were immunoprecipitated, and samples were analyzed by western blotting with anti-phosphotyrosine. Anti-Notch immunoprecipitate was loaded at four serial dilutions: 1:30, 1:10, 1:3 and undiluted. A family of high molecular weight bands is observed in the Notch IP (arrows) and bands of the same size are observed in anti-Dab and anti-Trio IPs. (Bottom) The same filter was stripped and reprobed with anti-Notch to document that the anti-phosphotyrosine signal in the top panel comigrates with Notch. Quantification of relative co-IP efficiency for phosphorylated Notch versus total Notch by serial dilution gave the same result in three independent experiments.

2008), a *Notch* derivative that is truncated at codon 2155 is fully active for *Notch*-dependent axon guidance. This form of the protein has only three tyrosines in the ICD. We therefore mutated all three tyrosines to phenylalanine (3YF), expressed the resulting derivative [$Notch^{\Delta 2155(3YF)}$] in neurons of $Notch^{ts1}$ embryos and assayed *Notch*-dependent axon patterning in the CNS and for ISNb. The activity of this derivative was reduced by 55% in terms of CNS longitudinal axon growth (quantified as the percentage of intersegment CNS longitudinal connections broken between neuromeres) and by 71% in terms of ISNb guidance (quantified as the percentage of abdominal hemisegments 2-7 with bypass defects) relative to the parent $UAS\text{-}Notch^{\Delta 2155(WT)}$ (Fig. 6A,B). By contrast, the same 3YF mutation of the canonically active Notch derivative $Notch^{\Delta 2268}$ shows no discernable impairment in regulation of neurogenesis (Fig. 6C): it suppresses the neurogenic phenotype of the strong allele $Notch^{55e11}$ as effectively as does the parent $Notch^{\Delta 2268(WT)}$ [although, to our surprise, the rescue of CNS neurogenesis by both of these derivatives was less complete than that of the equivalent construct lacking motifs 4 and 5 (compare with Fig. 4F), an observation that we explore in the Discussion].

To better quantify the activities of these modified *Notch* transgenes, we reanalyzed these same genotypes, but counted the number of neurons in an anatomically defined cell population, namely the dorsal cluster of sensory neurons in embryonic abdominal segments 1-7 (revealed by labeling with anti-Elav). Consistent with the qualitative results from anti-HRP staining, expression of $Notch^{\Delta 2268(3YF)}$ rescued neurogenesis as effectively as did $Notch^{\Delta 2268(WT)}$ (25.8±1.0 versus 27.1±0.9 dorsal sensory neurons per hemisegment; $P>0.3$, *t*-test), while $Notch^{\Delta 2268(\Delta 4\text{-}5)}$ was even more effective than $Notch^{\Delta 2268(WT)}$ at restoring neuron number (11.9±0.3 neurons per hemisegment) (Fig. 7A-E, quantified in F). Expression of the 3YF derivatives of $Notch^{\Delta 2268}$ and $Notch^{\Delta 2155}$ were equivalent to that of the wild-type and Δ4-5 forms of these proteins (Fig. 6D,E). We also verified by immunostaining that both $Notch^{\Delta 2268(\Delta 4\text{-}5)}$ and $Notch^{\Delta 2268(3YF)}$ are transported to the cell surface at least as effectively as $Notch^{\Delta 2268(WT)}$ *in vivo* (Fig. 7G-J, quantified in N), and are present in axons (Fig. 7K,L) and specifically in motoneuron growth cones (Fig. 7M).

We next tested the ability of $Notch^{\Delta 2155}$ derivatives to associate with Dab and Trio (Fig. 6E). To our surprise, we found that $Notch^{\Delta 2155(3YF)}$ co-precipitates with Dab and Trio about as well as does the parent protein. This shows that tyrosine phosphorylation of Notch is not required for binding the effectors Dab and Trio, but rather for binding some other, as yet unidentified, component, or else for a process subsequent to complex formation. Similarly, consistent with our previous studies of $Notch^{\Delta RamA}$, $Notch^{\Delta 2155(\Delta 4\text{-}5)}$ co-precipitates effectively with Dab and Trio, presumably reflecting the presence of a second Dab binding site on Notch [possibly in the ankryin repeats (Le Gall et al., 2008)], and accounting for the residual axonal activity of the Notch derivative lacking the motif 4-5 Dab binding site (Fig. 4C-E).

DISCUSSION

Notch controls axon patterning in the CNS and peripheral nervous system (PNS) of the *Drosophila* embryo, using a non-canonical signaling mechanism to locally suppress the activity of the Abl tyrosine kinase signaling pathway. Data presented here demonstrate that this signaling system shares with canonical Notch signaling a requirement for the ligand-induced S2 and S3 proteolytic cleavages of Notch, but unlike canonical signaling it also requires tyrosine phosphorylation of residues in the NICD in

Development (2018) 145, dev151548. doi:10.1242/dev.151548

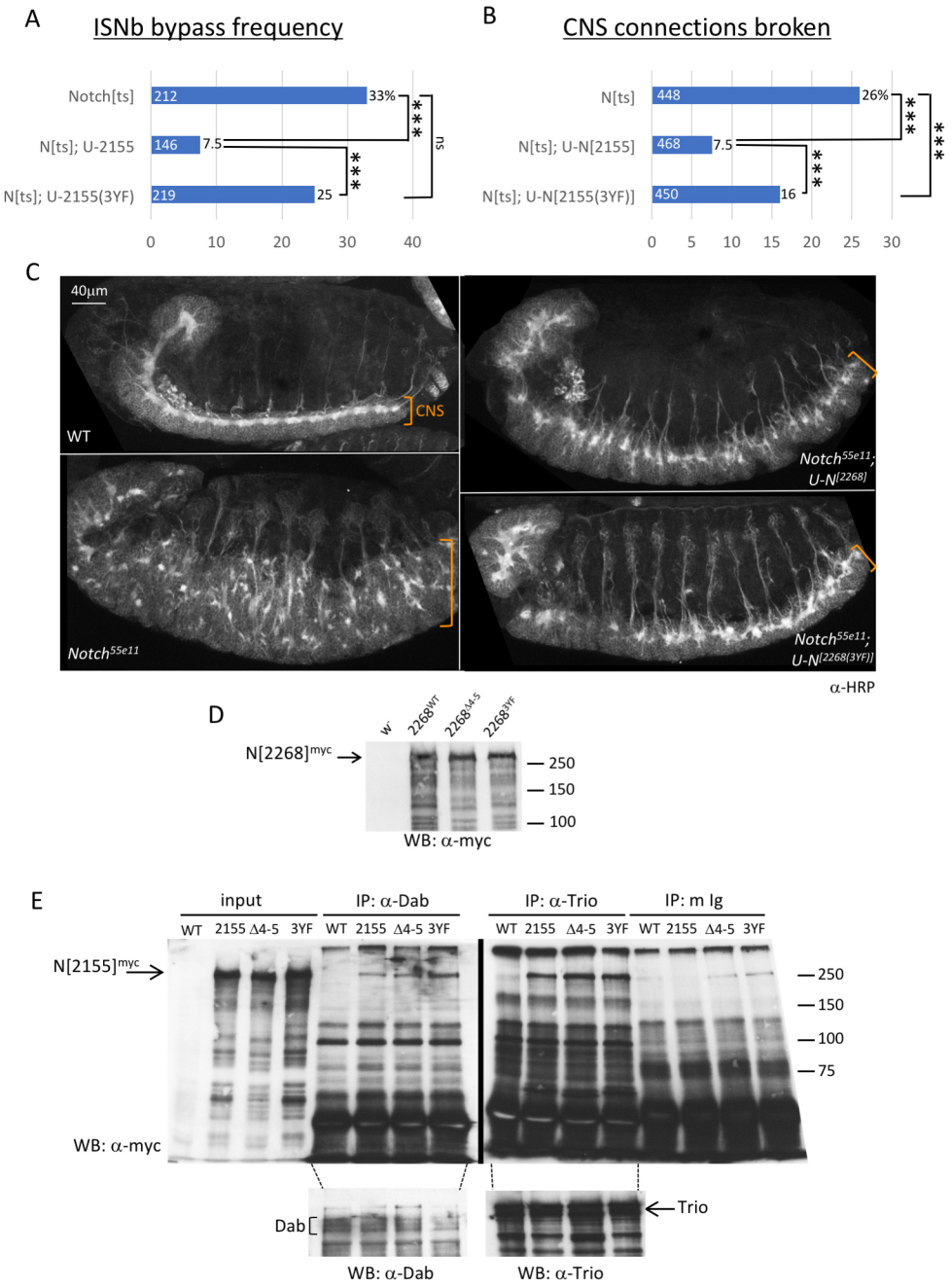

Fig. 6. Tyrosine residues in the Notch ICD are required for axon patterning activity, but not for neurogenesis or for binding to Dab and Trio. (A) Bypass frequency in abdominal hemisegments 2-7. Embryos were collected, subjected to temperature shift, fixed and immunostained with anti-Fasciclin 2. ISNb was visualized by Nomarski microscopy and quantified. ***P<0.001 (χ^2, with Bonferroni correction). n is indicated for each genotype (white numbers). Note that control data (*Notch^{ts}* and *Notch^{ts}; UAS-Notch$^{\Delta 2155}$*) report the same control samples shown in Fig. 4C. (B) Frequency of longitudinal axon tract breaks in embryo CNS, based on immunostaining with mAb BP102. ***P<0.001 (χ^2, with Bonferroni correction). Note that control data (*Notch^{ts}* and *Notch^{ts}; UAS-Notch$^{\Delta 2155}$*) report the same samples used for the control of Fig. 4E. (C) Lateral view of CNS in the indicated genotypes, visualized by immunofluorescence with anti-HRP. Orange bracket indicates thickness of nerve cord as a measure of neuron number. Transgene expression was driven with *P[sca-GAL4]*. Scale bar: 40 µm. (D) Anti-myc western of extract from control embryos (*w*–) or embryos expressing the indicated derivatives of myc-tagged *Notch$^{\Delta 2268}$* under the control of *sca-GAL4*. Molecular weight markers (kDa) are indicated; arrow points to full-length Notch$^{\Delta 2268\text{-myc}}$. (E) (Top) Anti-myc western of IPs from extracts of embryos that are wild type or that express the indicated Notch derivative. Samples were run simultaneously on two gels in the same apparatus (indicated by the vertical black bar) and the blots aligned based on markers. (Bottom) The filter on the left was stripped and reprobed with anti-Dab; the filter on the right was stripped and reprobed with anti-Trio. ECL exposure of these controls is shown aligned under the appropriate gel lanes (dotted lines), with Dab- and Trio-specific bands indicated.

order to regulate Abl. We also show that binding of Notch to Dab and Trio does not require ligand activation, but that full Notch activity does require a phylogenetically conserved protein motif in the juxtamembrane region of the NICD that contributes to binding and function of Dab, and is separate from the nearby N-terminal Su(H)-binding motif.

We show that a population of Notch protein molecules is phosphorylated on tyrosine residues *in vivo*, that this population is selectively associated with the Abl pathway components Dab and Trio, and that relevant tyrosines in the ICD are required for Notch axonal function as assayed by longitudinal axon growth in the CNS and guidance of ISNb in the PNS. Remarkably, however, these tyrosines are not required for association of Notch with its partners Dab and Trio. It might be that Notch tyrosine phosphorylation is required for a step in signaling after complex formation; for example, for proper subcellular localization or protein turnover after ligand activation. Perhaps consistent with this, there is a prior report of tyrosine phosphorylation of mouse Notch1 in cultured C2C12 myoblasts treated with a lysosomal inhibitor *in vitro* (Jehn et al., 2002). The physiological relevance, and functional significance, of this modification have never been established *in vivo* however. Alternatively, it might be that there is an additional, as yet unidentified, component of the Notch-Dab-Trio complex, and Notch tyrosine phosphorylation is required for the recruitment of that hypothetical component. Perhaps consistent with that speculation, our recent experiments ordering the steps in Abl signaling have independently generated biochemical hints of an additional component in Dab-Trio signaling complexes (Kannan et al., 2017). It is not clear which tyrosine kinase phosphorylates Notch *in vivo*. We do not think it is Abl itself, since overexpression

Development (2018) 145, dev151548. doi:10.1242/dev.151548

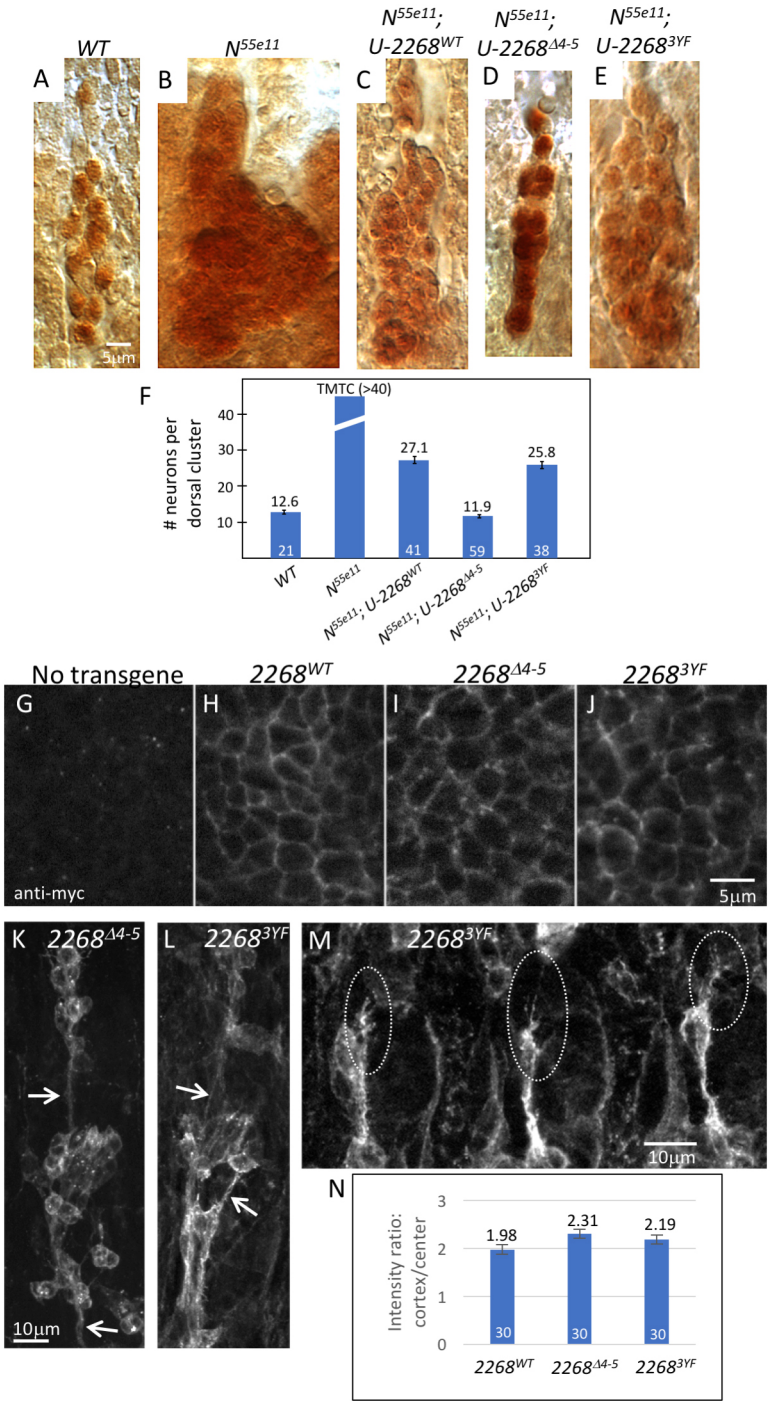

Fig. 7. Canonical signaling activity and subcellular localization of Notch$^{\Delta 2268}$ derivatives. (A-E) Embryos were fixed 12-14 h after egg laying (AEL), labeled with anti-Elav, processed with peroxidase histochemistry to reveal neuronal nuclei, and the dorsal cluster of abdominal sensory neurons counted. One representative cluster is shown in each panel. (F) Quantification of data from the experiment of A-E, showing mean (±s.e.m.) number of neurons per dorsal cluster. Wild-type embryo (A): 12.6±0.1 dorsal sensory neurons per abdominal hemisegment. *Notch^{55e11}* (B): estimated to be substantially >40 (too many to count, TMTC). *Notch^{55e11}; sca-GAL4; UAS-Notch$^{\Delta 2268(WT)}$* (C): 27.1±0.9. *Notch^{55e11}; sca-GAL4; UAS-Notch$^{\Delta 2268(\Delta 4\text{-}5)}$* (D): 11.9±0.3. *Notch^{55e11}; sca-GAL4; UAS-Notch$^{\Delta 2268(3YF)}$* (E): 25.8±1.0. *n* (hemisegments) is indicated in white. (G-M) The indicated *myc*-tagged *UAS-Notch* transgene was expressed in wild-type embryos under the control of *elav-GAL4*, embryos were fixed 9-14 h AEL, and transgene expression was visualized by immunofluorescence with anti-myc tag antibody. (G-J) Single optical section from a ventral view of the embryo CNS. (K-M) Maximum intensity projection of a *z*-stack of a lateral view of the embryo. Arrows (K,L) indicate peripheral nerves; dotted ovals (M) highlight growth cones of extending motor axons. (G) No *Notch* transgene. (H) *UAS-Notch$^{\Delta 2268(WT)}$*. (I) *UAS-Notch$^{\Delta 2268(\Delta 4\text{-}5)}$*. (J) *UAS-Notch$^{\Delta 2268(3YF)}$*. (K) *UAS-Notch$^{\Delta 2268(\Delta 4\text{-}5)}$*. (L) *UAS-Notch$^{\Delta 2268(3YF)}$*. (M) *UAS-Notch$^{\Delta 2268(3YF)}$*. (N) Quantification of data from the experiment of H-J. Integrated intensity of cortical immunofluorescent signal, and of cytoplasmic immunofluorescent signal, was measured for single CNS neurons of each genotype as described in the Materials and Methods, and the ratio of the signals calculated. Bars indicate the average value (±s.e.m.) of the ratio for 30 randomly selected cells. *n* (CNS neurons) is indicated in white. Scale bars: 5 µm in A-E,G-J; 10 µm in K-M.

of Abl does not enhance the phosphotyrosine immunoreactivity of Notch (data not shown). That experiment is not conclusive, however, and additional studies will be required. Moreover, we cannot rule out the possibility that additional phosphorylatable tyrosines exist in the most C-terminal portion of Notch (codons 2269-2703), which was not analyzed in this study.

Rather surprisingly, the Notch motif required for binding to the Dab PTB domain *in vitro* bears no resemblance to the usual PTB-binding homology NPXY (Smith et al., 2006), and indeed has no tyrosine residues at all. We do not have a structural picture for how the peptide defined by motifs 4 and 5 of the Notch Ram domain (Tamura et al., 1995) associates with the Dab PTB. It might be that some surface of the PTB domain besides the NPXY-binding cleft is responsible for association with Dab (Stolt et al., 2004; Yun et al., 2003). If so, it must be some phylogenetically conserved portion of the domain, as our initial Notch-Dab *in vitro* binding experiments were performed using the mouse Dab1 PTB domain in parallel with experiments employing the *Drosophila* Dab PTB (E.G., unpublished observations). We suspect that both motifs 4 and 5 contribute binding affinity to the interaction, as previous experiments have shown that the *Notch$^{\Delta A}$* deletion that removes motif 4 eliminates binding entirely, but clustered point mutations in either the N-terminal or C-terminal half of motif 4 reduce binding only modestly (C. de Mattei and E.G., unpublished). In our studies,

Development (2018) 145, dev151548. doi:10.1242/dev.151548

the reduction in Notch-Dab binding affinity from deletion of motifs 4 and 5 did not abolish the ability to detect complex formation by co-IP. Nonetheless, it was evidently sufficient to compromise regulation of Abl signaling substantially. It might be that suppression of Abl signaling by Notch requires some threshold level of Notch-Dab binding affinity that is not achieved by the $Notch^{\Delta 4\text{-}5}$ mutant. Alternatively, it might be that this mutation alters the conformation of the complex in a way that inhibits suppression of Abl activity.

We also tested for a role for Notch tyrosine phosphorylation in canonical signaling. We added back 113 codons (not including any tyrosines) to the 3′ end of $Notch^{\Delta 2155}$ to restore the C-terminal Su(H)-binding region and thereby restore partial canonical activity to this truncated form of Notch ($Notch^{\Delta 2268}$). Consistent with the biochemical finding that essentially all of the tyrosine-phosphorylated Notch was found in Dab-Trio complexes, $Notch^{\Delta 2268(3YF)}$ was equivalent to $Notch^{\Delta 2268(WT)}$ in its ability to rescue the neurogenic phenotype of a strong *Notch* allele. By contrast, $Notch^{\Delta 2268\Delta 4\text{-}5}$, which lacks the Dab binding site, actually appeared to be more active for canonical signaling than the parent $Notch^{\Delta 2268(WT)}$. The reason for this is unclear. Perhaps the canonical and Abl-dependent Notch pathways compete for a limited pool of activated Notch protein, with this competition becoming functionally limiting for *Notch* derivatives that are partially defective in signaling. If so, it might imply that absence of the Dab binding site reduces titration of Notch by the Abl-dependent pathway, thus increasing its availability to contribute to canonical signaling. By that model, tyrosine phosphorylation would presumably act at some later step in the signaling process. Alternatively, it might be that nuclear entry of cleaved NICD is limited by bound Dab. Additional experiments will be necessary to distinguish between these models.

Much of our functional analysis of *Notch* derivatives has employed artificial expression of truncated Notch proteins, which conceivably could produce non-physiological effects due to overexpression. Although this formal possibility cannot be excluded entirely, we observe very similar effects with many, very different derivatives, and the functions shown here are consistent with phenotypes observed with simple, classical genetic mutants of *Notch*, *Dab*, and their various partners (Crowner et al., 2003; Giniger, 1998; Giniger et al., 1993; Kuzina et al., 2011; Le Gall et al., 2008; Song et al., 2010). We therefore suggest that the data discussed here are likely to reveal bona fide features of Notch signaling.

Blocking Notch S2 cleavage, either by mutation of *rumi* or of the Rumi target sites on Notch, eradicates the ability of Notch to execute its axon patterning functions at elevated temperature. Rumi has not been exploited widely as a reagent to probe S2 cleavage of Notch. However, functional experiments have shown that the Rumi-dependent modifications of Notch are required subsequent to plasma membrane localization and Delta binding, but prior to S3 cleavage, and that they are required for S2 cleavage to occur (Acar et al., 2008). Formally, it is possible that Rumi modification affects some other essential process that Notch undergoes at precisely this time that has never been identified, but that seems unlikely. Moreover, while the various glycosylations of Notch can affect other aspects of receptor maturation, including its trafficking, for this purpose Rumi-dependent glucosylation is largely redundant with other forms of glycosylation, such as fucosylation (Ishio et al., 2015), such that if only Rumi modification is disturbed, Notch protein of adequate quantity and quality is displayed on the cell surface to perform all Notch functions at standard temperature (25°C) and, at elevated temperature, all functions before and after S2 cleavage. Finally, it has been speculated that Rumi may be involved in ‘quality control’ of Notch (Takeuchi et al., 2012). Even if this is correct, however, the data of Acar et al. (2008) argue strongly that the only functional deficit in Notch signaling upon disrupting Rumi-dependent glucosylation is simultaneous with S2 cleavage. We also found that hypomorphic axon patterning defects from partial reduction of *Notch* activity are enhanced substantially by heterozygous mutations of the S3 protease *Psn*. Together with experiments manipulating Rumi-dependent modification of Notch, these data demonstrate that both the S2 and S3 cleavages contribute significantly to Notch-dependent axonal regulation.

Based on the experiments above, we propose the following model for the mechanism by which Notch regulates Abl signaling (Fig. 8). Previous experiments show that Dab is an upstream activator of Abl kinase and Trio is an activator of Rac GTPase signaling (Kannan et al., 2017; Newsome et al., 2000). Notch, as shown here, binds to Dab and Trio in the absence of ligand activation. Upon binding of Delta to Notch, and consequent S2 and S3 cleavage, NICD is released from the membrane, taking with it Dab and Trio. Since Abl

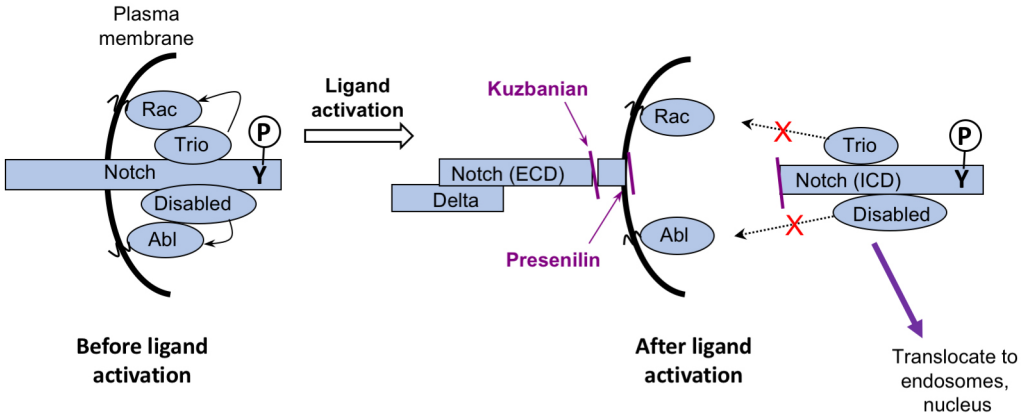

Fig. 8. Model for regulation of Abl signaling by Notch. Prior to ligand activation, Notch is bound to Dab and Trio. This population of Notch protein is phosphorylated on tyrosine (Y-P). Dab localizes Abl and stimulates its kinase activity (Kannan et al., 2017; Song et al., 2010); Trio stimulates Rac signaling. After binding to ligand (Delta) and proteolytic cleavage (Kuzbanian and Presenilin), Notch ICD is released from the plasma membrane and traffics away while remaining bound to Dab and Trio. This disrupts Abl signaling complexes (red X) by physically displacing the upstream regulatory components from their direct targets, thereby suppressing Abl pathway signaling.

Development (2018) 145, dev151548. doi:10.1242/dev.151548

and Rac are fatty-acylated and tethered to the membrane (Hantschel et al., 2003; Hodge and Ridley, 2016), release of NICD will thus disrupt Abl signaling complexes, separating the upstream regulators from their target downstream effectors. This will suppress both of the major branches of Abl signaling [the Abl-dependent inhibition of Enabled (Ena), and the activation of Trio/Rac, respectively (Kannan et al., 2017)], which our previous genetic experiments have shown to be the ultimate targets of Notch axonal signaling in fly embryos (Crowner et al., 2003). Together, these effects are expected to alter the ratio of linear to branched actin in the axonal growth cone (Kannan et al., 2017), modulate the function of the secretory apparatus (Kannan et al., 2014), and possibly modify linkage of axonal components to the microtubule cytoskeleton (Lee et al., 2004). The role of tyrosine phosphorylation in this schema is not yet clear; perhaps it plays a role in subcellular localization or turnover of NICD-Dab-Trio complexes (Jehn et al., 2002).

The model we propose also clarifies an apparent difference in how the Notch-Dab interaction manifests in *Drosophila* versus vertebrates. In the fly, Notch appears to act upstream of Dab and Abl, controlling their signaling in axons (Crowner et al., 2003), whereas in the migration of vertebrate cortical neurons it has been argued that mouse Dab1 acts upstream of Notch1 (Hashimoto-Torii et al., 2008; Keilani and Sugaya, 2008; Sibbe et al., 2009). It has been puzzling how such a fundamental property can differ in a conserved signaling pathway. What our model now proposes, however, is that Notch and Dab actually traffic together as they leave the plasma membrane. Which gene appears to act 'upstream' or 'downstream' will reflect whichever aspect of the pathway is limiting for the assay more than it does the nature of the signaling complex. Thus, in growth cone turning, the assay reports release of Dab (and Trio) from the membrane by cleavage of Notch, whereas in cortical neuron migration the assay reports the trafficking of NICD upon phosphorylation of Dab. In each case, however, the biology turns on the same molecular event, i.e. the concerted release of the Notch-Dab complex from the plasma membrane.

A key question raised by our experiments is whether the non-canonical Notch signaling mechanism we have dissected here is also used in other contexts, particularly in vertebrates. We initially identified the Dab binding site on Notch by virtue of its conservation in mammalian Notch sequences; indeed, homology motifs 4 and 5 were first noted in mammalian Notch (Tamura et al., 1995). Consistent with this, the Notch-Dab protein interaction has been validated in the mammalian nervous system as a key element of reelin signaling in lamination of the mammalian cortex (Hashimoto-Torii et al., 2008; Keilani and Sugaya, 2008; Sibbe et al., 2009). Although a role for Abl in this process has not been documented directly, both the Abl regulator Dab, and the Abl effector Ena, are required for cortical lamination (Goh et al., 2002; Howell et al., 1997). It thus seems plausible to suppose that Abl itself is also involved in the Notch-dependent migration of cortical neurons in the mammalian brain. In addition, there is also evidence for both Dab and the Abl effector Rac playing key roles in Notch-dependent apicobasal organization of the zebrafish neuroepithelium (Ohata et al., 2011). These data, together with the phylogenetic conservation of signaling mechanisms in general and Notch signaling in particular, make it extremely likely that the mechanism we have documented here also acts in vertebrate development.

MATERIALS AND METHODS

Genetics, *Drosophila* stocks and temperature-shift protocols

rumi alleles were obtained from Melih Acar (UT Southwestern, Dallas, TX, USA). Flies bearing *Notch* transgenes lacking Rumi modification sites were constructed and generously provided by Hamed Jafar-Nejad and colleagues (Baylor College of Medicine, Houston, TX, USA). In brief, *Notch* genomic clones, inserted in the *P[acman]* vector, were modified by site-directed mutagenesis via recombineering and integrated into the genome with *ϕC31* recombinase, as described in detail by Leonardi et al. (2011). Psn^{C2} was from Gary Struhl (Columbia University, New York, NY, USA). All other *Drosophila* lines were either previously published lab stocks, new transformant lines (described below) or were obtained from the Bloomington *Drosophila* Stock Center (BDSC). All experiments employing *P[w+; elav-GAL4]* were performed with the second chromosome insertion of this transgene.

Germline clones of $rumi^{26}$ were obtained by crossing $hs\text{-}FLP^{122}$*; FRT[82B] rumi*^{26}*/balancer* females to males that were *w; FRT[82B] P[w+;ovo*^{D1}*]* to generate progeny that included the female genotype *w/hs-FLP*^{122}*; FRT[82B] rumi*^{26}*/FRT[82B] P[w+;ovo*^{D1}*]*. These were heat shocked at first larval instar (37°C, 30 min), collected as adults, and crossed to males that were *rumi*^{26}*/TM3 P[actin-lacZ]*. Embryos were collected, subjected to temperature shift (see below), fixed and immunostained by standard methods.

Temperature-shift experiments were performed as described previously (Crowner et al., 2003; Le Gall et al., 2008). For analyzing ISNb phenotypes ($Notch^{ts1}$ and *rumi* experiments), embryos were collected for 3 h at 18°C, aged for 12 h at 18°C, shifted for 6 h at 32°C and fixed. For analyzing $Notch^{ts1}$ CNS phenotypes with mAb BP102, embryos were collected for 3 h at 18°C, aged for 8 h at 18°C, shifted for 6 h at 32°C and fixed. Temperature-shift treatments of embryos were performed on coverslips bearing a thin layer of grape juice agar, using an MJ Research PTC100 PCR machine with slide griddle. For co-IP experiments with $Notch^{ts1}$ extracts, adult flies were shifted to 32°C for at least 24 h before isolating heads and making extracts; embryos were shifted for at least 4 h.

Antibodies, embryo fixation and immunostaining

Antibodies were as follows: anti-phosphotyrosine (4G10, EMD-Millipore; 1:1000 for western), mouse anti-myc tag (mAb 9E10, Thermo Scientific; 1:2000 for western), rabbit anti-myc tag (#C3956, Sigma Aldrich; 1:1000 for embryo staining) and anti-β-galactosidase (#0855976, MP Biomedicals; 1:1000 for embryo staining). The following antibodies were from the Developmental Studies Hybridoma Bank: anti-Fasciclin 2 (1D4; 1:50 for embryo staining), anti-Sxl (M114; 1:100 for embryo staining), mAb BP102 (1:50 for embryo staining), anti-Disabled (P4D11 for IP, 0.9 ml per IP; P6E11 for western, 1:3), anti-Trio (9.4A, concentrate; 1:150 for western; 0.075 ml per IP), anti-Notch (C17.9C6, supernatant; 1:300 for western; ascites, 0.019 ml per IP) and rat anti-Elav (7E8A10, supernatant; 1:2).

All secondary antibodies, rabbit anti-mouse antibody, non-immune mouse IgG and TRITC-labeled anti-HRP (1:150 for embryo staining) were from Jackson ImmunoResearch. For anti-Eve staining, biotinyl-TSA (Thermo Scientific) enhancement was applied, and visualized with FITC-streptavidin, as described previously (Kuzina et al., 2011). Peroxidase histochemistry used Vectastain Elite ABC (Vector Labs) per manufacturer's protocol. Biotinyl-TSA enhancement was also used for detection of anti-Elav labeling, visualized by peroxidase histochemistry with Vectastain Elite.

Embryo fixation, staining and mounting were by standard methods (Crowner et al., 2003; Le Gall et al., 2008). Embryo neurogenic phenotypes were assessed in whole-mounts in Vectashield (Vector Labs) using a Zeiss 880 confocal microscope. Axonal phenotypes of peroxidase-labeled embryos were assessed in filet mounts in 70% glycerol using a Zeiss Axioskop 2 with Nomarski optics. For purposes of presentation, image planes of fluorescently labeled samples were combined as maximum intensity projections and image planes of peroxidase-labeled samples were montaged, as required. Statistical significance of embryo phenotypes was assessed by χ^2 test, with Bonferroni correction. Values for *n* and for percent affected are displayed on the graphs for all samples. Embryo genotypes were inferred from absence of expression of *lacZ* marker genes borne on appropriate balancer chromosomes. Marked balancers used in this work were: *FM7C B P[actin-lacZ]*, *Cy P[actin-lacZ]*, *CyO P[engrailed-lacZ]*, *TM3 Sb P[actin-lacZ]* and *TM6B Tb Hu P[Ubx-lacZ]*; all are available from BDSC. In some experiments, $Notch^{ts1}$ homozygous female parents were used to generate embryos, and *Notch* hemizygous male progeny were identified by lack of labeling with anti-Sxl antibody.

Development (2018) 145, dev151548. doi:10.1242/dev.151548

Relative cortical versus intracellular localization of myc-tagged *Notch* transgenes was quantified as follows. Embryos bearing the indicated transgenes were fixed and immunostained with rabbit anti-myc and FITC-anti-rabbit antibodies, as described above, and image stacks of the CNS were obtained with a Zeiss Axioimager microscope using the Apotome module. Single optical sections were then analyzed in ImageJ. For each genotype, 30 CNS neurons were selected randomly (ten from each of three different embryos). For each selected cell, the cortical immunofluorescent signal was traced manually in ImageJ and the integrated intensity of the cortical signal was determined. For the same cell, a subcortical ring was then traced manually, and the integrated intensity of the area located within the subcortical ring was determined. The ratio of these measurements was then calculated, and the mean and standard error of the ratio for each genotype was calculated in Excel (Microsoft).

Biochemical methods

Embryo and adult extract preparation and immunoprecipitation were performed as described previously (Le Gall et al., 2008). Note that use of the complete panel of specified protease inhibitors is essential to prevent proteolysis of Dab and Trio. Phosphatase treatment was performed with calf intestine phosphatase (New England Biolabs) for 30 min at 37°C in 25 mM Tris pH 7.5, 100 mM NaCl in the presence of protease inhibitors. Western detection was by Lumigen ECL Ultra (Lumigen). Preparation of GST-Disabled PTB, *in vitro* translation of Notch derivatives, GST pulldown and autoradiographic visualization were as described previously (Giniger, 1998; Le Gall and Giniger, 2004). For all biochemical experiments, results shown in figures were reproduced in multiple, independent experiments.

Transgene descriptions and transformation

Plasmid constructions were prepared by standard methods. Mutations were introduced either by PCR mutagenesis or by the QuikChange method (Agilent Technologies). *Notch* modifications were as follows. (1) The *Δ4/5* mutation deletes codons R1790-S1811, inclusive. (2) The three tyrosines mutated to phenylalanine in the $Notch^{3YF}$ mutation are Y1850, Y1860 and Y2097. (3) Sequences encoding $Notch^{\Delta 2155}$ were subcloned into the *Bam*HI site of pCS2-MT (a gift from Dave Turner and Rafi Kopan), in frame with the C-terminal 6×myc epitope tag. $Notch^{\Delta 2268}$ was then generated by restoring codons 2156-2268 as a PCR product. (4) $FLAG\text{-}Notch^{\Delta E}$ is essentially the same as $Notch^{\Delta E}$ described by Larkin et al. (1996), with the signal sequence and signal cleavage site of *Delta* fused to N1742 of *Notch*, and with *Notch* truncated at codon K2236, but with an oligonucleotide encoding a single FLAG tag inserted between the signal cleavage site and the first *Notch* codon. (5) $FLAG_3\text{-}Notch^{\Delta 2155}$ was generated from *UAS-*$FLAG_3$*-Notch1779* (Le Gall and Giniger, 2004) by truncation of the *Notch* sequence at the *Bam*HI site (codon 2155) and replacing the 3′ end of the *Notch* gene with an oligonucleotide encoding a stop codon.

All Notch subcloning and mutagenesis were performed in pBluescript (Invitrogen) and pCS2-MT. Reconstructed *Notch* genes were introduced into pUAS-T and transformed into *w* or *yw Drosophila* (BestGene). We note the following unexpected phenotypes of some transgenes, the causative mechanisms of which are unknown: (1) while $Notch^{\Delta 2155}$ transgenes had no detectable canonical Notch activity in the background of a strong or null *Notch* mutation, in a wild-type background they derepressed the endogenous locus, producing Notch gain-of-function phenotypes in multiple tissues (e.g. bristle to socket transformations in the notum); (2) the expression of $Notch^{\Delta 2268\text{-}myc(WT)}$ in neurons with *elav-GAL4* had no obvious deleterious effects, whereas expression of $Notch^{\Delta 2268\text{-}myc(\Delta 4\text{-}5)}$ or $Notch^{\Delta 2268\text{-}myc(3YF)}$ with *elav-GAL4* was almost fully lethal prior to adult eclosion.

Acknowledgements

We are grateful to all the members of our lab who have contributed to these experiments, particularly J. K. Song, Cory DeMattei, Dan Crowner, Ginger Hunter and Maude LeGall. We thank Hamed Jafar-Nejad, Melih Acar and Gary Struhl for the gift of fly stocks; and Stephen Wincovitch of the NHGRI Microscopy Core for assistance with confocal microscopy. The Bloomington *Drosophila* Stock Center (Indiana University, Bloomington, IN, USA) provided essential *Drosophila* stocks, and the Developmental Studies Hybridoma Bank (University of Iowa, Iowa City, IA, USA) provided essential antibody reagents.

Competing interests

The authors declare no competing or financial interests.

Author contributions

Conceptualization: R.K., L.W., E.G.; Investigation: R.K., E.C., L.W., I.K., Q.G., E.G.; Writing - original draft: E.G.; Writing - review & editing: R.K., E.C., L.W., E.G.; Supervision: E.G.; Project administration: E.G.; Funding acquisition: E.G.

Funding

Early portions of this work were supported by National Institutes of Health grant R01 GM57830 to E.G., and the balance by intramural funds of the Basic Neuroscience Program of the National Institute of Neurological Disorders and Stroke (NINDS) Intramural Research Program (Z01 NS003013) to E.G. R.K. was supported in part by a Ramalingaswami re-entry fellowship from the Department of Biotechnology, Ministry of Science and Technology, Government of India. Deposited in PMC for release after 12 months.

References

Acar, M., Jafar-Nejad, H., Takeuchi, H., Rajan, A., Ibrani, D., Rana, N. A., Pan, H., Haltiwanger, R. S. and Bellen, H. J. (2008). Rumi is a CAP10 domain glycosyltransferase that modifies Notch and is required for Notch signaling. *Cell* **132**, 247-258.

Andersen, P., Uosaki, H., Shenje, L. T. and Kwon, C. (2012). Non-canonical Notch signaling: emerging role and mechanism. *Trends Cell Biol.* **22**, 257-265.

Androutsellis-Theotokis, A., Leker, R. R., Soldner, F., Hoeppner, D. J., Ravin, R., Poser, S. W., Rueger, M. A., Bae, S.-K., Kittappa, R. and McKay, R. D. G. (2006). Notch signalling regulates stem cell numbers in vitro and in vivo. *Nature* **442**, 823-826.

Coleman, H. A., Labrador, J.-P., Chance, R. K. and Bashaw, G. J. (2010). The Adam family metalloprotease Kuzbanian regulates the cleavage of the roundabout receptor to control axon repulsion at the midline. *Development* **137**, 2417-2426.

Crowner, D., Le Gall, M., Gates, M. A. and Giniger, E. (2003). Notch steers *Drosophila* ISNb motor axons by regulating the Abl signaling pathway. *Curr. Biol.* **13**, 967-972.

Fambrough, D., Pan, D., Rubin, G. M. and Goodman, C. S. (1996). The cell surface metalloprotease/disintegrin Kuzbanian is required for axonal extension in Drosophila. *Proc. Natl. Acad. Sci. USA* **93**, 13233-13238.

Fuerstenberg, S. and Giniger, E. (1998). Multiple roles for notch in Drosophila myogenesis. *Dev. Biol.* **201**, 66-77.

Giniger, E. (1998). A role for *abl* in *Notch* signaling. *Neuron* **20**, 667-681.

Giniger, E. (2012). Notch signaling and neural connectivity. *Curr. Opin. Genet. Dev.* **22**, 339-346.

Giniger, E., Jan, L. Y. and Jan, Y. N. (1993). Specifying the path of the intersegmental nerve of the Drosophila embryo: a role for Delta and Notch. *Development* **117**, 431-440.

Goh, K. L., Cai, L., Cepko, C. L. and Gertler, F. B. (2002). Ena/VASP proteins regulate cortical neuronal positioning. *Curr. Biol.* **12**, 565-569.

Greenwald, I. and Kovall, R. (2013). Notch signaling: genetics and structure. *WormBook* 1-28, doi: 10.1895/wormbook.1.10.2.

Hansson, E. M., Lendahl, U. and Chapman, G. (2004). Notch signaling in development and disease. *Semin. Cancer Biol.* **14**, 320-328.

Hantschel, O., Nagar, B., Guettler, S., Kretzschmar, J., Dorey, K., Kuriyan, J. and Superti-Furga, G. (2003). A myristoyl/phosphotyrosine switch regulates c-Abl. *Cell* **112**, 845-857.

Hashimoto-Torii, K., Torii, M., Sarkisian, M. R., Bartley, C. M., Shen, J., Radtke, F., Gridley, T., Šestan, N. and Rakic, P. (2008). Interaction between Reelin and Notch signaling regulates neuronal migration in the cerebral cortex. *Neuron* **60**, 273-284.

Hattori, M., Osterfield, M. and Flanagan, J. G. (2000). Regulated cleavage of a contact-mediated axon repellent. *Science* **289**, 1360-1365.

Hayward, P., Brennan, K., Sanders, P., Balayo, T., DasGupta, R., Perrimon, N. and Martinez Arias, A. (2005). Notch modulates Wnt signalling by associating with Armadillo/beta-catenin and regulating its transcriptional activity. *Development* **132**, 1819-1830.

Hodge, R. G. and Ridley, A. J. (2016). Regulating Rho GTPases and their regulators. *Nat. Rev. Mol. Cell Biol.* **17**, 496-510.

Howell, B. W., Hawkes, R., Soriano, P. and Cooper, J. A. (1997). Neuronal position in the developing brain is regulated by mouse disabled-1. *Nature* **389**, 733-737.

Ishio, A., Sasamura, T., Ayukawa, T., Kuroda, J., Ishikawa, H. O., Aoyama, N., Matsumoto, K., Gushiken, T., Okajima, T., Yamakawa, T. et al. (2015). O-fucose monosaccharide of *Drosophila* Notch has a temperature-sensitive function and cooperates with O-glucose glycan in Notch transport and Notch signaling activation. *J. Biol. Chem.* **290**, 505-519.

Jehn, B. M., Dittert, I., Beyer, S., von der Mark, K. and Bielke, W. (2002). c-Cbl binding and ubiquitin-dependent lysosomal degradation of membrane-associated Notch1. *J. Biol. Chem.* **277**, 8033-8040.

Kannan, R., Kuzina, I., Wincovitch, S., Nowotarski, S. H. and Giniger, E. (2014). The Abl/Enabled signaling pathway regulates Golgi architecture in Drosophila photoreceptor neurons. *Mol. Biol. Cell* **25**, 2993-3005.
Kannan, R., Song, J.-K., Karpova, T., Clarke, A., Shivalkar, M., Wang, B., Kotlyanskaya, L., Kuzina, I., Gu, Q. and Giniger, E. (2017). The Abl pathway bifurcates to balance Enabled and Rac signaling in axon patterning in Drosophila. *Development* **144**, 487-498.
Keilani, S. and Sugaya, K. (2008). Reelin induces a radial glial phenotype in human neural progenitor cells by activation of Notch-1. *BMC Dev. Biol.* **8**, 69.
Kopan, R. and Ilagan, M. X. G. (2009). The canonical Notch signaling pathway: unfolding the activation mechanism. *Cell* **137**, 216-233.
Kuzina, I., Song, J. K. and Giniger, E. (2011). How Notch establishes longitudinal axon connections between successive segments of the Drosophila CNS. *Development* **138**, 1839-1849.
Labrador, J. P., O'Keefe, D., Yoshikawa, S., McKinnon, R. D., Thomas, J. B. and Bashaw, G. J. (2005). The homeobox transcription factor even-skipped regulates netrin-receptor expression to control dorsal motor-axon projections in Drosophila. *Curr. Biol.* **15**, 1413-1419.
Larkin, M. K., Holder, K., Yost, C., Giniger, E. and Ruohola-Baker, H. (1996). Expression of constitutively active Notch arrests follicle cells at a precursor stage during Drosophila oogenesis and disrupts the anterior-posterior axis of the oocyte. *Development* **122**, 3639-3650.
Lee, H., Engel, U., Rusch, J., Scherrer, S., Sheard, K. and Van Vactor, D. (2004). The microtubule plus end tracking protein Orbit/MAST/CLASP acts downstream of the tyrosine kinase Abl in mediating axon guidance. *Neuron* **42**, 913-926.
Le Gall, M. and Giniger, E. (2004). Identification of two binding regions for the suppressor of hairless protein within the intracellular domain of Drosophila notch. *J. Biol. Chem.* **279**, 29418-29426.
Le Gall, M., De Mattei, C. and Giniger, E. (2008). Molecular separation of two signaling pathways for the receptor, Notch. *Dev. Biol.* **313**, 556-567.
Lehmann, R., Jimenez, F., Dietrich, U. and Campos-Ortega, J. A. (1983). On the phenotype and development of mutants of early neurogenesis in Drosophila melanogaster. *Wilehm Roux Arch. Dev. Biol.* **192**, 62-74.
Leonardi, J., Fernandez-Valdivia, R., Li, Y.-D., Simcox, A. A. and Jafar-Nejad, H. (2011). Multiple O-glucosylation sites on Notch function as a buffer against temperature-dependent loss of signaling. *Development* **138**, 3569-3578.
Lieber, T., Kidd, S., Alcamo, E., Corbin, V. and Young, M. W. (1993). Antineurogenic phenotypes induced by truncated Notch proteins indicate a role in signal transduction and may point to a novel function for Notch in nuclei. *Genes Dev.* **7**, 1949-1965.
Newsome, T. P., Schmidt, S., Dietzl, G., Keleman, K., Åsling, B., Debant, A. and Dickson, B. J. (2000). Trio combines with dock to regulate Pak activity during photoreceptor axon pathfinding in Drosophila. *Cell* **101**, 283-294.
Ohata, S., Aoki, R., Kinoshita, S., Yamaguchi, M., Tsuruoka-Kinoshita, S., Tanaka, H., Wada, H., Watabe, S., Tsuboi, T., Masai, I. et al. (2011). Dual roles of Notch in regulation of apically restricted mitosis and apicobasal polarity of neuroepithelial cells. *Neuron* **69**, 215-230.
Perumalsamy, L. R., Nagala, M., Banerjee, P. and Sarin, A. (2009). A hierarchical cascade activated by non-canonical Notch signaling and the mTOR-Rictor complex regulates neglect-induced death in mammalian cells. *Cell Death Differ.* **16**, 879-889.
Rebay, I., Fehon, R. G. and Artavanis-Tsakonas, S. (1993). Specific truncations of Drosophila Notch define dominant activated and dominant negative forms of the receptor. *Cell* **74**, 319-329.
Selkoe, D. and Kopan, R. (2003). Notch and Presenilin: regulated intramembrane proteolysis links development and degeneration. *Annu. Rev. Neurosci.* **26**, 565-597.
Sibbe, M., Forster, E., Basak, O., Taylor, V. and Frotscher, M. (2009). Reelin and Notch1 cooperate in the development of the dentate gyrus. *J. Neurosci.* **29**, 8578-8585.
Smith, M. J., Hardy, W. R., Murphy, J. M., Jones, N. and Pawson, T. (2006). Screening for PTB domain binding partners and ligand specificity using proteome-derived NPXY peptide arrays. *Mol. Cell. Biol.* **26**, 8461-8474.
Song, J. K., Kannan, R., Merdes, G., Singh, J., Mlodzik, M. and Giniger, E. (2010). Disabled is a bona fide component of the Abl signaling network. *Development* **137**, 3719-3727.
Stolt, P. C., Vardar, D. and Blacklow, S. C. (2004). The dual-function disabled-1 PTB domain exhibits site independence in binding phosphoinositide and peptide ligands. *Biochemistry* **43**, 10979-10987.
Struhl, G. and Greenwald, I. (1999). Presenilin is required for activity and nuclear access of Notch in Drosophila. *Nature* **398**, 522-525.
Takeuchi, H., Kantharia, J., Sethi, M. K., Bakker, H. and Haltiwanger, R. S. (2012). Site-specific O-glucosylation of the epidermal growth factor-like (EGF) repeats of Notch: efficiency of glycosylation is affected by proper folding and amino acid sequence of individual EGF repeats. *J. Biol. Chem.* **287**, 33934-33944.
Tamura, K., Taniguchi, Y., Minoguchi, S., Sakai, T., Tun, T., Furukawa, T. and Honjo, T. (1995). Physical interaction between a novel domain of the receptor Notch and the transcription factor RBP-J kappa/Su(H). *Curr. Biol.* **5**, 1416-1423.
Wills, Z., Bateman, J., Korey, C. A., Comer, A. and Van Vactor, D. (1999). The tyrosine kinase Abl and its substrate enabled collaborate with the receptor phosphatase Dlar to control motor axon guidance. *Neuron* **22**, 301-312.
Wilson, J. J. and Kovall, R. A. (2006). Crystal structure of the CSL-Notch-Mastermind ternary complex bound to DNA. *Cell* **124**, 985-996.
Yun, M., Keshvara, L., Park, C.-G., Zhang, Y.-M., Dickerson, J. B., Zheng, J., Rock, C. O., Curran, T. and Park, H.-W. (2003). Crystal structures of the Dab homology domains of mouse disabled 1 and 2. *J. Biol. Chem.* **278**, 36572-36581.
Zecchini, V., Brennan, K. and Martinez-Arias, A. (1999). An activity of Notch regulates JNK signalling and affects dorsal closure in Drosophila. *Curr. Biol.* **9**, 460-469.